Available online at www.sciencedirect.com
SCIENCE DIRECT®
Journal of Power Sources 140 (2005) 400–408
JOURNAL OF POWER SOURCES
www.elsevier.com/locate/jpowsour

Analysis of an automatic energy recovery system for partially spent batteries

Roger A. Dougal, Zhenhua Jiang*, Lijun Gao

Department of Electrical Engineering, University of South Carolina, Columbia, SC 29208, USA

Received 22 July 2004; accepted 19 August 2004
Available online 14 October 2004

Abstract

This paper analyzes the performance of a system for automatic recovery and consolidation of energy from partially spent batteries. The objective for this system is to minimize the stockpile of batteries needed to run a suite of portable electronic devices on a daily, mission-oriented, basis. This system adapts to various battery types and allows the user to conveniently choose between charging and discharging specific batteries without changing the battery positions. The control algorithm is able to automatically select which secondary batteries should preferentially be charged. The control algorithm also continuously adjusts the discharging current of each battery according to its estimated state-of-charge. This concept is then verified by numerical simulation in the Virtual Test Bed (VTB) environment, which shows that the system is able to recover most of the energy from several partially spent batteries simultaneously. The effects of the discharge rate of the batteries on the overall system efficiency and the total discharging time are discussed.

Keywords: Virtual Test Bed; State-of-charge; Partially spent batteries

1. Introduction

Batteries play a critical role in the propagation and utilization of portable electronic devices such as portable computers, cellular phones, cameras, camcorders, MEMS, CD/MP3 players and radios, and are now nearly essential in the daily lives of civilians and military personnel [1–3]. For a long-term trip or military mission, the people or military personnel may need to carry many batteries to power the many portable electronic devices they use. One of their objectives is to find a way to minimize the number of individual batteries that they have to carry to support all of their equipment. Some items of equipment use different batteries than others, and every item discharges the batteries at a different rate. So if a person wants to minimize the weight for a 1-day mission, they would take partially spent batteries out of their equipment and replace them with fresh batteries. But then the energy in the partially spent batteries would be wasted. For example, a person might have two AA alkaline batteries, each at 25% state-of-charge (SOC), one D size alkaline battery at 30% SOC, and a lithium-ion battery at 20% SOC. None of these batteries can power their respective loads for a full day, yet they do contain useful energy. A simple way to recover the residual energy is to use the two AA alkaline batteries and the D size alkaline battery to recharge the lithium-ion battery, thereby consolidating all of the energy into one battery. The objective of our work, then, is to develop and assess the effectiveness of an energy recovery system that can automatically reclaim and consolidate energy from partially spent batteries (either primary or secondary batteries) into secondary batteries.

Ideally, the energy recovery system should be able to automatically adapt to any type of battery put into the “source” side, and any other type of rechargeable battery put into the “load” side. In general, the initial states of the batteries being inserted will be considerably different [4]. A battery with higher initial state-of-charge may require a larger discharging current or otherwise a longer discharging time. In order

* Corresponding author. Tel.: +1 803 777 9314; fax: +1 803 777 8045.
E-mail address: jiang@engr.sc.edu (Z. Jiang).

0378-7753/$ – see front matter © 2004 Elsevier B.V. All rights reserved.
doi:10.1016/j.jpowsour.2004.08.034

to extract as much energy as possible, the discharge rate will have to decrease as the source battery becomes more deeply depleted [5]. Therefore, an interesting but difficult part in the automatic energy recovery system is controlling the current drawn from the partially depleted batteries so as to extract nearly all of the available energy within the shortest period. Another point of interest is how to choose which secondary batteries to charge from the many ones available, based on the total charge available. State-of-charge is a measure of the charge remaining in the battery but it is difficult to measure directly [6]. Many people have studied methods for state-of-charge estimation. Liu et al. presented two methods in [7] both of which have drawbacks; the ampere-hours method requires information about the initial state-of-charge, and the recursive method needs a lot of offline experimental data to obtain the many parameters. In our application, we adopt a simple and practical approach based on the measured battery current and voltage. While not highly accurate, it is sufficient for the rough estimates needed for this application.

In the following, we present the system and control designs for the automatic battery energy recovery system. This system can put nearly all of the energy from batteries on the "source" side into the rechargeable batteries on the "load" side. The concept is then verified by numerical simulation and the results are presented. The effects of the discharge rate of the batteries on the overall system efficiency and the total discharging time are discussed.

2. System design

In general, the battery energy recovery system should allow to automatically attract energy from multiple partially spent batteries and to put the energy into multiple partially spent secondary batteries on a continuous basis, and it should be possible to insert any battery at any time. The case of five bi-directional charging/discharging channels is studied in this paper, which can represent the general solution of many channels.

Fig. 1 illustrates the system which is self-powered from the batteries inserted into it. The system consists of five individual, identical charging/discharging channels and an integrated controller. Power can flow through any power converter in either direction. The user can choose between charging and discharging their battery by setting the controller. The high voltage side of each power converter is connected to a common voltage bus so that all power converters have the same voltage at the high voltage side. The power converters control the charging/discharging currents of each battery, and allocate the available power among the batteries. The controller coordinates the individual power converters. The currents and voltages of the batteries are sensed and fed into the controller which calculates the reference charging/discharging current for each channel and the corresponding duty cycle, and then generates the actual PWM switching signals for the power converters.

3. Control system development

The control system manages the discharging process, selects which batteries should be charged, regulates the bus voltage, and limits the charging currents and voltages. In order to achieve high system efficiency, a floating bus voltage strategy is applied. The bus voltage is set at 1.2 times the highest voltage of any battery so that the power converters operate at high efficiency which results from a small voltage change in the converter. One objective of the power converters responsible for charging the batteries is to maintain this floating bus voltage. If any charging current exceeds the safe charging limit for a battery, then the power converter is regulated to output a constant current that equals the safe charging limit. If the voltage of any battery being charged exceeds the voltage limit, the output voltage of the power converter will be kept constant and equal to the voltage limit. Whenever all of the charging currents or voltages exceed their safe limits, the controller will reduce the discharge rate of the batteries being discharged.

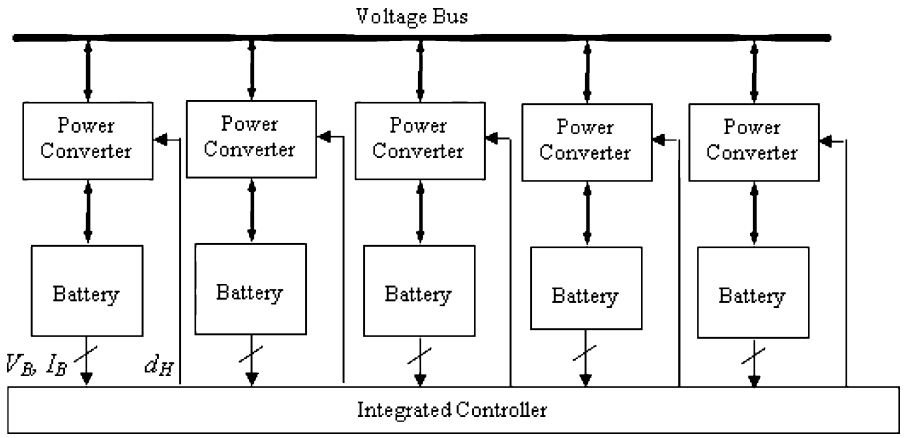

Fig. 1. Block diagram of the proposed automatic energy recovery system.

3.1. Discharging strategy

Let us first consider a basic relationship between the charge level of the battery and the discharging current. The charge of the battery can be expressed as follows [8]:

$$C_{\text{end}} = C_{\text{r}}\,\text{SOC}_0 - \int_0^{t_{\text{end}}} I\,\text{d}t \tag{1}$$

where C_{r} is the rated capacity of the battery (A h), SOC_0 the initial state-of-charge, I the discharging current in magnitude (A), t_{end} the total discharging time (h). In Eq. (1), the term $C_{\text{r}}\,\text{SOC}_0$ represents the initial charge remaining in the battery. From Eq. (1), it is seen that the remaining charge of the battery is the integral of the discharging current over the total discharging time until the battery is fully depleted. If we use direct currents of the same magnitude to discharge two different batteries, the discharging time will be approximately (neglecting nonlinearity) proportional to the charge remaining in the battery. This means that the discharging time will be approximately proportional to the state-of-charge for two batteries of equal capacity, or proportional to the capacity of two batteries at the same state-of-charge. If we want all the batteries to become fully discharged during the same period of time, the discharging current can be made proportional to the charge level of the partially spent battery that is equal to the capacity times the state-of-charge. Therefore, the discharging current for the battery can be calculated according to

$$I_i = k_{\text{disc}} k_i C_{\text{r},i}\,\text{SOC}_i \tag{2}$$

where I_i is the discharging current of the ith battery (A), $C_{\text{r},i}$ the rated capacity of the ith battery (A h), SOC_i the state-of-charge of the ith battery, k_i a constant specific to the battery that represents the state-of-health of the battery, and k_{disc} the discharge rate constant that is identical to all batteries. The discharging strategy can adjust the discharging currents continuously according to the estimated state-of-charge of each battery.

3.2. Charging strategy

As mentioned previously, the control system should automatically select which of the secondary batteries should be charged. The charging strategy aims to select the less depleted secondary batteries to charge first because then it takes less time to fill as many batteries as possible. The charge that is needed to fill each battery is equal to the product of the rated capacity and the depth-of-discharge (calculated as unity minus the state-of-charge). Assume that there are M secondary batteries to be charged. The charge needed by each battery is arranged in ascending order and denoted as CHARGE [k], where k = 1, 2, . . ., M. The batteries are then numbered from #1 to #M in this order, which means that, among these batteries, battery #1 will need the least charge to become full. If the total available charge (denoted by CHARGE_SUM) is less than that needed by the least depleted battery (#1), the charging strategy will select this battery to charge. If the total available charge is more than that needed by the least depleted battery (#1) but less than that needed by both #1 and #2, the charging strategy will select to charge these two batteries. But the charging order depends on the charge needed by #2. If the charge needed by #2 is more than the total available charge, the strategy selects to first charge #1 and then charge #2 so that the first battery will be ready within the shortest time. Otherwise, both batteries are charged simultaneously. In this case, both batteries will have a final charge level at least higher than 50%. This charging pattern is followed by the rest of the controllers for the other batteries. The charging strategy is described as follows:

```
IF CHARGE_SUM < CHARGE [1]
    Charge battery #1
ELSE IF CHARGE_SUM < CHARGE [1] + CHARGE [2]
    IF CHARGE_SUM < CHARGE [2]
      Charge #1 and then charge #2 after #1 finished
    ELSE
      Charge #1 & #2 simultaneously
    END
. . .. . .
ELSE IF CHARGE_SUM < CHARGE [1] + CHARGE [2]
  + . . . + CHARGE [M]
    IF CHARGE_SUM < CHARGE [M]
      Charge #1, #2, . . ., #M − 1 simultaneously,
        and then charge #M
    ELSE
      Charge #1, #2, . . ., #M simultaneously
    END
ELSE
    Charge #1, #2, . . ., #M simultaneously
END
```

3.3. State-of-charge estimation

In the charging and discharging strategies, the discharging current varies with the state-of-charge of the battery, and the total charge available is calculated based on the state-of-charge estimates. Obviously, the state-of-charge is important information for the control algorithm. Since it is impossible to measure the state-of-charge directly, a method should be found to estimate it from the measured voltage and current of the battery. Since there is an approximately fixed nonlinear relationship between the state-of-charge and open-circuit voltage [9], we estimate the state-of-charge from the battery voltage according to a piecewise linear relation, as shown in Fig. 2a. The voltage space is divided into 10 zones and the

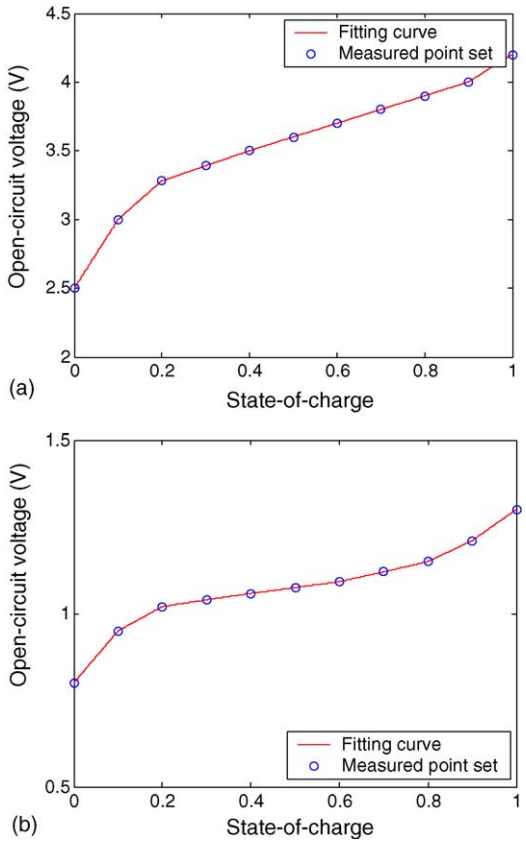

Fig. 2. Piecewise-linear fitting between the open-circuit voltage and the state-of-charge of the battery. (a) Example voltage vs. state-of-charge curve for a lithium-ion cell; (b) an example of one NiH_2 cell.

open-circuit voltages are measured under the conditions that the state-of-charge is 0, 0.1, 0.2, . . ., 1.0. The voltage versus state-of-charge relation is then represented by 10 straight-line segments. When the open-circuit voltage falls within any zone, the estimate of the state-of-charge is obtained by means of linear interpolation between the two boundaries. The estimate is described in the following equation:

$$\text{SOC} = \frac{v_0 - a_i}{b_i} + c_i, \quad v_i < v_0 < v_{i+1},\ i = 0, 1, ..., 10 \tag{3}$$

where v_i and v_{i+1} are, respectively, the lower-limit and upper-limit of the open-circuit voltage within each zone, a_i, b_i and c_i are constants and they can be easily obtained from values v_i and v_{i+1}, v_0 is the battery open-circuit voltage. The lower-limit (v_i) corresponds with the condition that the state-of-charge is equal to $i \times 10\%$. The upper-limit (v_{i+1}) corresponds with the condition that the state-of-charge is equal to $(i + 1) \times 10\%$.

The voltage corresponding to each state-of-charge value, for instance, 0.1, can be obtained by measuring the open-circuit voltage when charging the battery to the corresponding charge level (i.e., 10%). The state-of-charge of the battery is decided using the following approach. Each battery is discharged to full depletion. A constant current is then applied

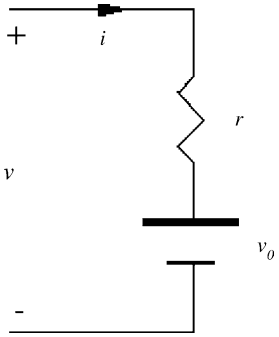

Fig. 3. Equivalent circuit for estimation of the open-circuit voltage of the battery.

to charge the battery until it is full and the total charging time is recorded. After fully depleting this battery, charging this battery with the same current for a proportion (equal to the state-of-charge in magnitude) of the total charging time can obtain a desired state-of-charge. This method ignores aging issues that cause a battery to have less capacity after many charge/discharge cycles than it had when new. For different type of batteries, the voltage versus state-of-charge curves may be different (for example, see Fig. 2b). It is possible to obtain a series of parameters for different batteries from some major manufactures through the same set of experiments. These parameters can be preset in the controller. When the users select their battery type, the corresponding parameter set will be used for the state-of-charge estimation.

In order to estimate the open-circuit voltage, we use a very simple model of the battery as shown in Fig. 3. Although it is not practical to directly measure the open-circuit voltage of the battery which is connected to the voltage bus, the internal potential of the battery is equal to the terminal voltage when the battery is open, which does not change with the external voltage being imposed across it at this moment.

From Fig. 3, it is clear that the open-circuit voltage of the battery, v_0, can be estimated from the following equation:

$$v_0 = v - ir \tag{4}$$

where v and i are the measured battery voltage and charging current, respectively; r the equivalent series resistance (ESR) of the battery. This current correction term is important to the state-of-charge estimate when the initial conditions of the batteries are widely disparate.

3.4. Control implementation

The control algorithm is then coded and modeled in the VTB. The main functional modules include the state-of-charge estimation module, the charging pattern select module, the discharging current strategy module, the current/voltage regulation module, and the discharging/charging termination decision module, as shown in Fig. 4.

In the charging pattern select module, the batteries to be charged are selected with the objective of appropriately allocating the total available charge that is calculated according

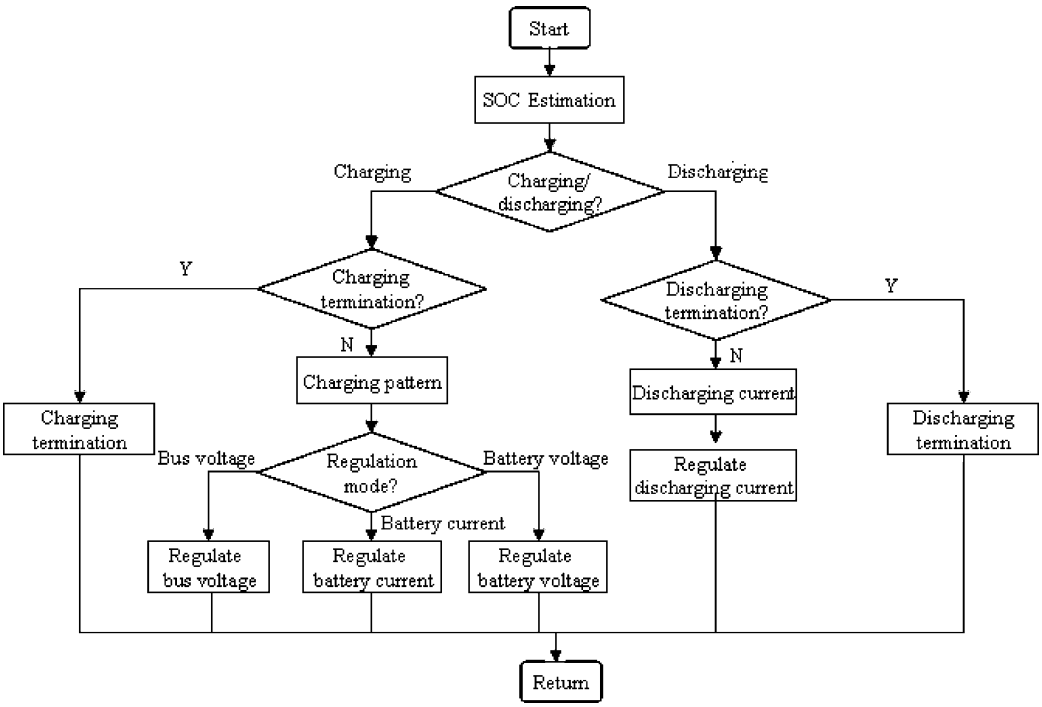

Fig. 4. Flow chart of the control algorithm.

to the estimated state-of-charge and the capacity that is input by the user. (This could be automated if each battery presented a battery identification code at its connection port.) The discharging current strategy module is to calculate the reference discharging currents according to the proposed current sharing algorithm, which is shown in Eq. (2). The current and voltage regulation modules are used to compute the duty cycles to the power converters according to the reference currents and voltages, respectively. The proportional–integral approach is used to regulate the currents and voltages. The regulation of the discharging current is formulated in the following equation:

$$d = d_{\text{old}} + k_{\text{p,idisc}}(I_{\text{disc,ref}} - I_{\text{disc}}) + k_{\text{i,idisc}} \int (I_{\text{disc,ref}} - I_{\text{disc}})\,\mathrm{d}t \quad (5)$$

where d and d_{old} are the current and previous duty cycles used to control the power converter; I_{disc} the discharging current of the battery; $I_{\text{disc,ref}}$ the reference discharging current of the battery; $k_{\text{p,idisc}}$, $k_{\text{i,idisc}}$ the proportional and integral gains for discharging current regulation, respectively. The bus voltage regulation is formulated as follows:

$$d = d_{\text{old}} + k_{\text{p,vbus}}(V_{\text{bus,ref}} - V_{\text{bus}}) + k_{\text{i,vbus}} \int (V_{\text{bus,ref}} - V_{\text{bus}})\,\mathrm{d}t \quad (6)$$

where I, V are the charging current and voltage of the battery, respectively; $V_{\text{bus,ref}}$ the reference bus voltage; $k_{\text{p,vbus}}$, $k_{\text{i,vbus}}$ the proportional and integral gains for bus voltage regulation, respectively. The charging current and voltage regulations of the secondary battery are formulated in Eqs. (7) and (8), respectively:

$$d = d_{\text{old}} + k_{\text{p}i}(I_{\text{ref}} - I) + k_{ii} \int (I_{\text{ref}} - I)\,\mathrm{d}t \quad (7)$$

$$d = d_{\text{old}} + k_{\text{p}v}(V_{\text{ref}} - V) + k_{iv} \int (V_{\text{ref}} - V)\,\mathrm{d}t \quad (8)$$

where I, V are the charging current and voltage of the battery, respectively; I_{ref} and V_{ref} the reference charging current and voltage of the battery, respectively; $k_{\text{p}i}$, k_{ii}, and $k_{\text{p}v}$, k_{iv} the proportional and integral gains for battery current and voltage regulations, respectively.

The discharging/charging termination decision module determines when the discharging/charging process should stop.

4. System modeling and simulation

A simulation model of the automatic battery energy recovery system was built in the Virtual Test Bed (VTB) environment [10]. The control algorithm has been discussed in the previous section. The models for batteries and power converters are briefly described below.

Various types of batteries can be used in this system. The objective of modeling the batteries is to replicate the electrical and thermal properties of the batteries as they interact with the external circuit. In this application, all electrochemical reactions are considered uniform throughout each porous electrode and all spatial variations of chemical concentrations

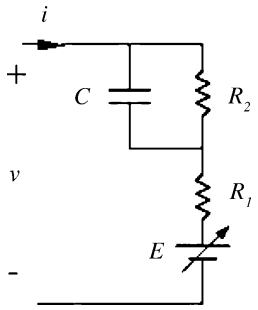

Fig. 5. Equivalent circuit of lithium-ion battery based on experimental data.

and potentials are ignored. The models are obtained by fitting the data from manufacturers' data sheets or independent measurements. Here, we take the lithium-ion battery model as an example to explain how to model the many types of batteries. The equivalent electrical schematic of the lithium-ion battery model is shown in Fig. 5.

The equivalent model comprises three components: an equilibrium potential E, an internal resistance that is divided into two components R_1 and R_2, and an effective capacitance C that represents localized storage of chemical energy within the porous electrodes. The equilibrium potential of the battery depends on the temperature and the amount of active material available in the electrodes, which can be specified in terms of depth of discharge. The potential E, the terminal voltage v and the depth of discharge (DOD) are related by the following equations:

$$i(t) = \frac{1}{R_2}[v(t) - E[i(t), T(t), t] - R_1 i(t)] + C\frac{\mathrm{d}}{\mathrm{d}t}[v(t) - E[i(t), T(t), t] - R_1 i(t)] \quad (9)$$

$$v[i(t), T(t), t] = \sum_{j=0}^{N} c_j \,\mathrm{DOD}^j[i(t), T(t), t] + \Delta E[T(t)] \quad (10)$$

$$\mathrm{DOD}[i(t), T(t), t] = \frac{1}{Q_\mathrm{r}}\int_0^t \alpha[i(\tau)]\beta[T(\tau)]i(\tau)\,\mathrm{d}\tau \quad (11)$$

where i is the battery current (A), N the highest order of the fitting polynomial of the reference curve, c_j the coefficient of the jth order term in the polynomial representation, and Q_r the battery capacity referred to the cutoff voltage for the reference curve (A h), T the battery temperature (K), t the independent time variable (s). A potential correction term $\Delta E(T)$ is used to compensate for the variation of equilibrium potential that is induced by the temperature change at the reference rate. The dependence of the depth of discharge on the rate is accounted for by a factor $\alpha(i)$. A factor $\beta(T)$ is used to account for the dependence of the depth of discharge on the temperature. The detail of how to determine these parameters can be found in [11].

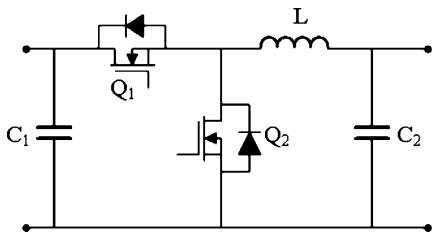

Fig. 6. Diagram of the bi-directional dc/dc converter (left: high voltage side, right: low voltage side).

Fig. 6 schematically shows the circuit diagram of a bi-directional dc/dc converter. The power converter consists mainly of a high side switch Q_1 and a complementary low side switch Q_2 (operating as a synchronous rectifier for the buck converter mode or as a main switch for the boost converter mode). This configuration is chosen due to the simplicity and high efficiency. The power inductor L stores energy and filters the ripple in the current. The capacitors C_1 and C_2 smooth the ripple in the input or output voltage.

Since the goal of the system-level simulation is to investigate the current sharing in the energy system and to monitor the main parameters of the system, the simulation time step can be long, for example, higher than 100 ms. In this case, an average-value model of the power converter is used and the switching transients are neglected. Fig. 7 illustrates the switching-average model of the bi-directional dc/dc converter accounting for the power loss. The power loss (including conduction loss and switching loss) in the power converter is represented by a loss resistor that consumes the same energy as that lost in the operation during each switching period. To get the power loss, efficiencies of the power converter at different power outputs can be measured. The loss resistance is expressed in the following equation:

$$R_\mathrm{on} = \frac{(1-\eta)V_\mathrm{H}I_\mathrm{H}}{I_\mathrm{H}^2} = (1-\eta)\frac{V_\mathrm{H}}{I_\mathrm{H}} \quad (12)$$

where η is the efficiency of the power converter under the condition that the high side voltage is constant at 20 V; V_H and V_L are the average voltages on the high voltage side and low voltage side of the converter, respectively; I_H the magnitude of the current flowing into or out of the high voltage side. Fig. 8 shows a measurement of efficiency of the power converter as a function of power at the high voltage side under the condition that the high side voltage is constant at 20 V.

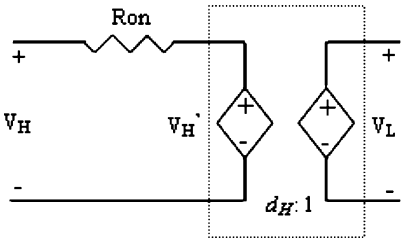

Fig. 7. Switching-average model of the bi-directional dc/dc converter accounting for the power loss.

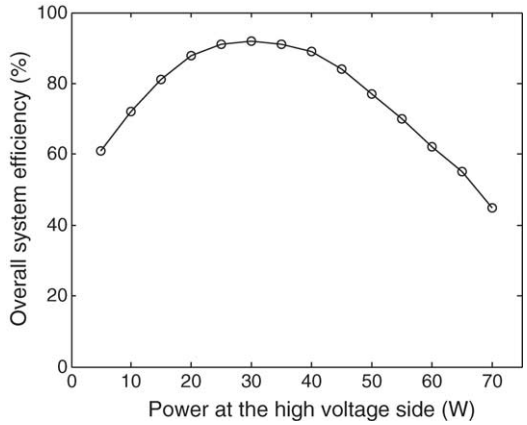

Fig. 8. Efficiency of the power converter as a function of power at the high voltage side under the condition that the high side voltage is constant at 20 V.

The power flow in the power converter is controlled by adjusting the ON/OFF duty cycle of the switches. The average low side voltage and high side voltage of the power converter is determined by the following equation:

$$\frac{V_{\mathrm{L}}}{V'_{\mathrm{H}}} = \frac{t_{\mathrm{on}}}{T} = d_{\mathrm{H}} \tag{13}$$

where V'_{H} is the ideal voltage on the high voltage side without considering the power loss, t_{on} the turn-on time of the switch on the high voltage side during a period, T the switching period, d_{H} the duty cycle of the PWM switching signal to the high side switch.

Fig. 9 shows the VTB schematic view of the system illustrated in Fig. 1. It consists of five channels: the first three for discharging the primary batteries, the latter two for charging the secondary batteries. While the primary batteries are 10 × 10 (series by parallel connections) array of Zn-air cells, 4 × 2 primary lithium cells, and one $LiSO_2$ cell (BA5590, 15 V/15 A h), respectively, the secondary batteries are 4 × 3 Li-ion cells and 4 × 2 Li-ion cells, respectively. For convenience, the batteries are numbered #1 through #5. The capacities of the batteries are 10 × 0.4, 2 × 1.4, 1 × 12, 3 × 1.5, and 2 × 1.5 A h, respectively. The initial states of charge of the primary batteries are 0.45, 0.3, and 0.2, respectively. The initial states of charge of the secondary batteries are 0.3 and 0.35, respectively. The constant k_i in Eq. (2) is, respectively, 1.0, 1.0 and 0.8 for batteries #1 to #3. The discharge rate constant k_{disc} in Eq. (2) is 1.0.

5. Results and discussion

The simulation is run for 2 h (7200 s), and the simulation results are shown in Figs. 10–13. Figs. 10 and 11 show the voltages and currents of the batteries, respectively. The state-

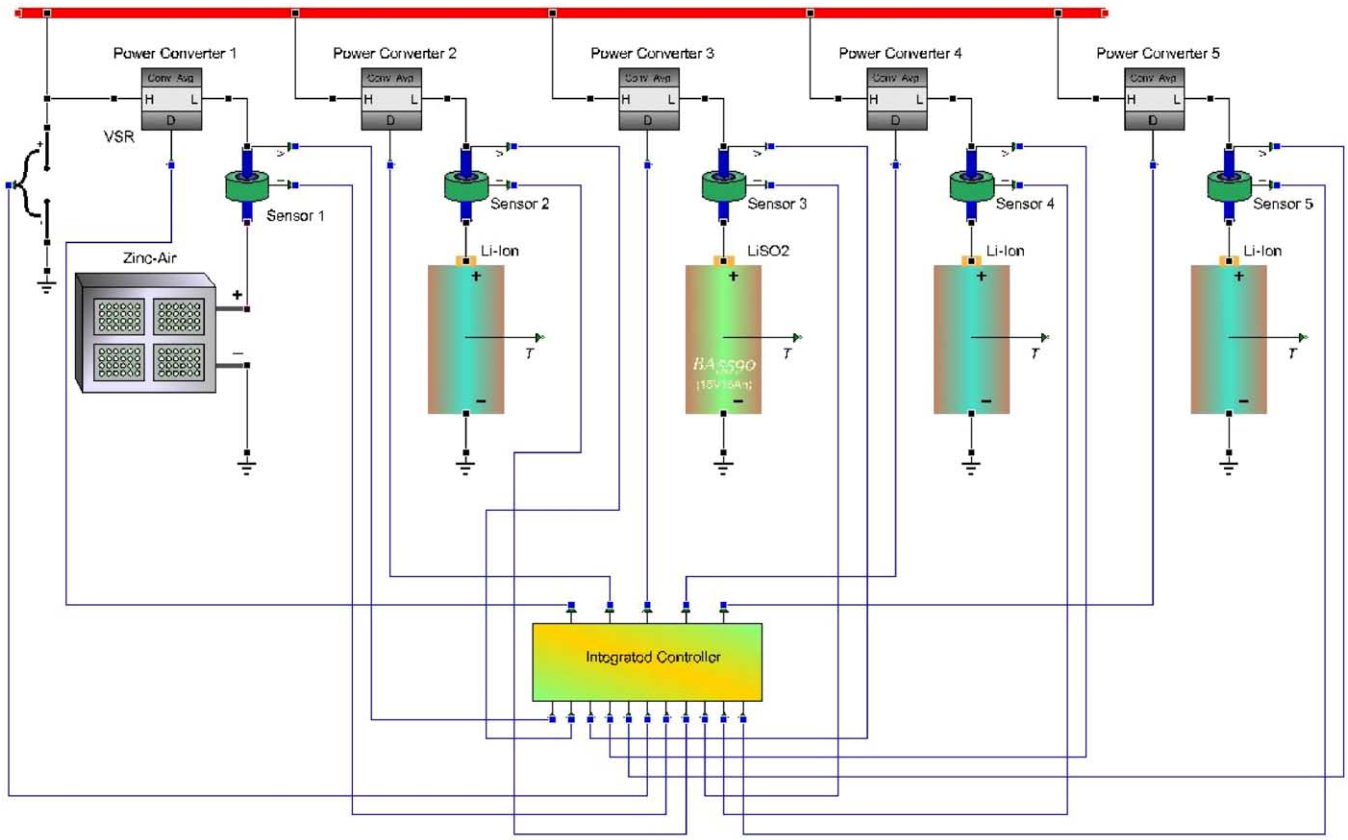

Fig. 9. VTB schematic view of the automatic energy recovery system for partially spent batteries.

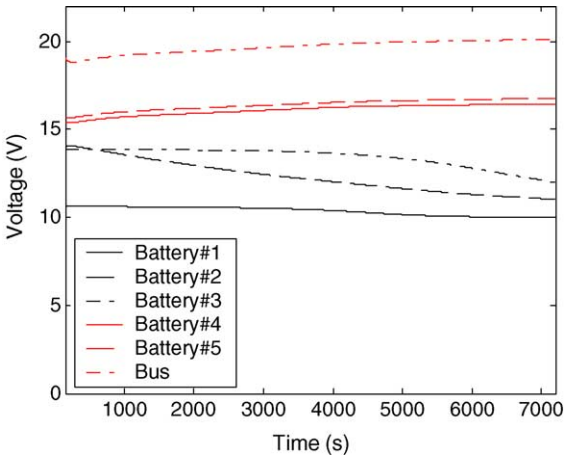

Fig. 10. Voltages of the batteries.

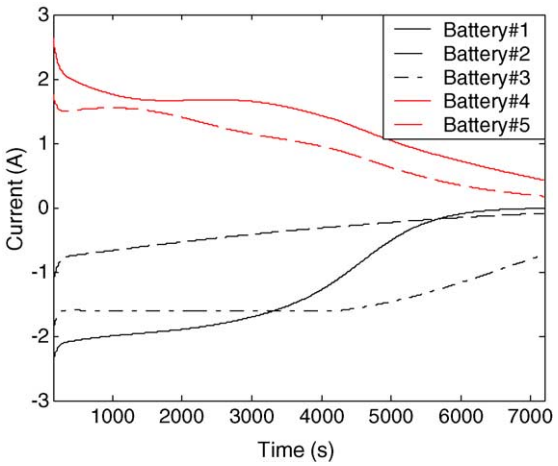

Fig. 11. Charging currents of the batteries.

of-charge of each battery is plotted in Fig. 12. Fig. 13 shows the duty cycles of the power converters.

Among these batteries, battery #5 has the highest voltage. It is shown in Fig. 10 that the bus voltage is higher than

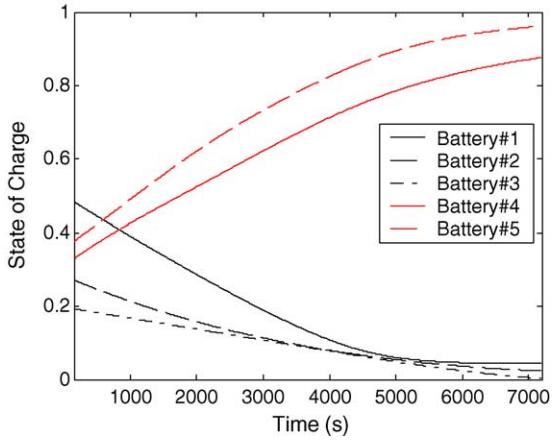

Fig. 12. State-of-charge of the batteries.

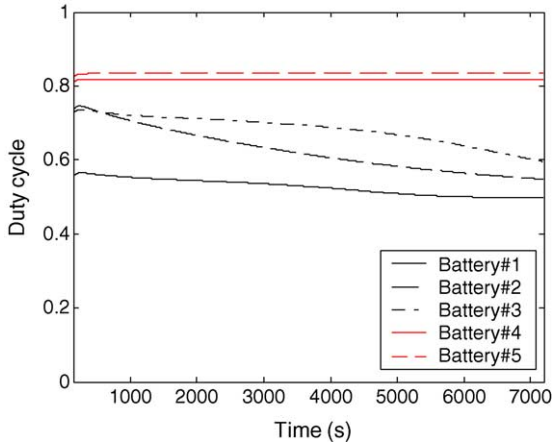

Fig. 13. Duty cycles of the power converters.

the voltages of all batteries and is 20% higher than the voltage of battery #5. The duty cycle of the power converter in series with battery #5 is around 0.8, as shown in Fig. 13. The voltages of batteries #1 through #3 decrease while the voltages of batteries #4 and #5 increase during the charging/discharging process. Consequently, the bus voltage increases with the voltage of battery #5, and the duty cycles of the power converters in the discharging channels decrease, as shown in Fig. 13. It is seen from Fig. 11 that the battery with the highest effective charge (state-of-charge times the capacity times state-of-health) is discharged at the highest current. The discharging currents vary with the estimates of state-of-charge and decrease with the charge of the batteries. The charging currents of the other two batteries decrease with time because the discharging currents (thus the power to charge the batteries) decrease. Fig. 12 shows that the state-of-charge increases when the battery is charged and decreases when the battery is discharged. The state-of-charge of battery #1 decreases more rapidly than the others because it has the lowest discharge capacity although its discharge rate is lower than the others. It is also shown that three discharging batteries get almost fully discharged after 2 h. At the end, two rechargeable batteries are charged to 86% and 95% charge levels, respectively. It is seen from the study that more than 80% of the available energy is recovered from the primary batteries.

System efficiency and discharging time are two parameters of concern to the user. They are dependent on the discharge rates of the batteries. Fig. 14 shows the effect of the discharge rate on the overall system efficiency that is a measure of the ratio of the energy transferred to the secondary batteries to the energy extracted from the partially depleted batteries. It is seen that a satisfactory overall system efficiency can be gained when the discharge rate constant is around 1.0 (i.e., k_{disc} is between 0.7 and 1.2). When the discharge rate is extremely high or low, the overall system efficiency decreases. This is because the power converter efficiency decreases when the power transferred is far away from the rated power at which the power converter is optimized. The best

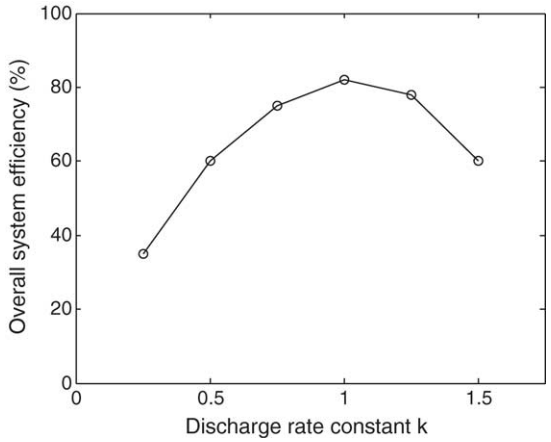

Fig. 14. Effect of the discharge rate on the overall system efficiency.

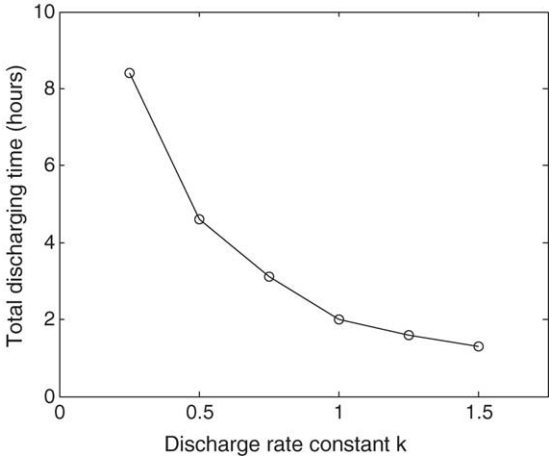

Fig. 15. Effect of the discharge rate on the total discharging time.

system efficiency could be obtained for a specific discharge rate by optimizing the power converters for the corresponding operating condition. Fig. 15 shows the effect of the discharge rate on the total discharging time. Obviously, the total discharging time decreases with the discharge rate. However, more energy could be extracted from the mostly depleted battery at a lower discharge rate. Tradeoff must be made to recover as much energy as possible within a limited time frame.

6. Conclusion

This paper describes the operating characteristics of a system for automatic recovery and consolidation of energy from partially spent batteries. The objectives for this system are to minimize the daily battery load carried by an individual, from a battery depot, to run all of the portable electronic devices necessary to accomplish remote tasks, and furthermore to minimize the stock requirements of the battery depot. This system adapts to various battery types and allows the user to conveniently choose between charging and discharging specific batteries. The control algorithm is able to automatically select which secondary batteries should preferentially be charged. The charging strategy aims to select the less depleted secondary batteries to charge first because it then takes less time to fill the first batteries. The control algorithm also continuously adjusts the discharging current of each battery according to its estimated state-of-charge that is obtained by estimating the battery open-circuit voltage with current correction and piecewise-linearly fitting between the open-circuit voltage and the state-of-charge. The bus voltage is regulated at a floating level (rather than at a fixed level) to obtain better system efficiency. This concept has been verified by numerical simulation in the Virtual Test Bed (VTB) environment. Simulation results show that the proposed system is able to recover most of the energy from several partially spent batteries simultaneously. The effects of the discharge rate on the overall system efficiency and the total discharging time have been discussed.

Acknowledgements

This work was supported by the US Office of Naval Research under grant N000140310952.

References

[1] R.J. Brodd, Overview: rechargeable battery systems, in: Proceedings of the Conference Record of WESCON'93, 1993, pp. 206–209.
[2] F. Putois, Market for nickel–cadmium batteries, J. Power Sources 57 (1) (1995) 67–70.
[3] S. Megahed, B. Scrosati, Lithium-ion rechargeable batteries, J. Power Sources 51 (1) (1994) 79–104.
[4] Z. Jiang, R. Dougal, Design and testing of a fuel-cell-powered battery-charging station, J. Power Sources 115 (2) (2003) 148–153.
[5] P. Ruetschi, Aging mechanisms and service life of lead-acid batteries, J. Power Sources 127 (1) (2004) 33–44.
[6] Z. Jiang, R. Dougal, Strategy for active power sharing in a fuel-cell-powered charging station for advanced technology batteries, in: Proceedings of the IEEE Power Electronics Specialists Conference, vol. 1, Acapulco, Mexico, 15–19 June 2003, pp. 81–87.
[7] T. Liu, D. Chen, C. Fang, Design and implementation of a battery charger with state-of-charge estimator, Int. J. Electron. 87 (2) (2000) 211–226.
[8] Z. Jiang, R. Dougal, Control design and testing of a novel fuel-cell-powered battery-charging station, in: Proceedings of the IEEE Applied Power Electronics Conference, Miami, FL, 9–13 February 2003, pp. 1127–1133.
[9] S. Piller, M. Perrin, A. Jossen, Methods for state-of-charge determination and their applications, J. Power Sources 96 (1) (2001) 113–120.
[10] T. Lovett, A. Monti, E. Santi, R. Dougal, A multilanguage environment for interactive simulation and development of controls for power electronics, in: Proceedings of the IEEE 32nd Annual Power Electronics Specialists Conference, vol. 3, 2001, pp. 1725–1729.
[11] L. Gao, S. Liu, R. Dougal, Dynamic lithium-ion battery model for system simulation, IEEE Trans. Compon. Packag. 25 (3) (2002) 495–505.